Composites Part B 125 (2017) 227–240

Contents lists available at ScienceDirect

Composites Part B

journal homepage: www.elsevier.com/locate/compositesb

Three-dimensional thermo-elastic analysis and dynamic response of a multi-directional functionally graded skew plate on elastic foundation

Mahdi Adineh, Mehran Kadkhodayan*

Department of Mechanical Engineering, Ferdowsi University of Mashhad, Mashhad, Iran

ARTICLE INFO

Article history:
Received 28 November 2016
Received in revised form
24 May 2017
Accepted 25 May 2017
Available online 30 May 2017

Keywords:
Skew plate
Differential quadrature method
Three–dimensional thermo-elasticity
Multi-directional functionally graded materials

ABSTRACT

Three-dimensional thermo-elastic analysis of a multi-directional functionally graded skew plate on elastic foundation under thermo-mechanical loading is carried out for the first time. Numerical results of displacement and stresses are obtained using differential quadrature method (DQM). Some material properties of the plate assumed to be temperature-dependent and graded in all three spatial directions according to a power law function. The results for various boundary conditions are obtained and the effects of grading index of material properties, temperature distribution, elastic foundation parameters and angle of skew plate are presented. Moreover, the dynamic response of a multi-directional functionally graded material skew plate on elastic foundation is obtained using 4D DQM for the first time. The results show that the material grading direction has a noticeable effect on plate behavior especially for the plates under thermal loading as well as for the dynamic response of the plate.

1. Introduction

The concept of functionally graded materials (FGMs) was introduced by Japanese researches at 1984 [1]. FGMs are a new generation of advanced composite materials in which the mechanical properties vary smoothly and continuously in one or more directions [2]. Hence, the composition of several different materials can be used in these structural components in order to optimize the responses of structures subjected to thermal and mechanical loading [3]. The analysis of FGM structures is an interesting and important subject and has attracted the attention of researchers in the last years [4–22].

Plates are well known structures with a wide application in many industries. Rectangular [23–34] and non-rectangular plates [35–37] such as skew plates [38–43] have been widely studied by researches in the literature. Most of researches have used plate theories to analysis the skew plates [39–43] and only few of them used the three-dimensional theory of elasticity. For example Zhou et al. [38] performed a free vibration analysis for a homogeneous skew plate using three-dimensional elasticity theory.

Several research works (such as [44–48]) have investigated the thermo-elastic analysis of FGM plates. However, thermo-mechanical behavior of FGM skew plates on elastic foundation has been studied rarely.

Joodaky and Joodaky [49] presented an approximate closed-form solution for static behavior of thin skew plates with various boundary conditions rested on Winkler and Pasternak foundations based on elasticity and neutral surface theories of FGMs. The assumed plate was subjected to a uniform load and the Extended Kantorovich Method (EKM) was used together with the idea of weighted residual technique to convert the governing fourth order partial differential equation (PDE) to two ordinary differential equations (ODEs). Lei et al. [50] used the element-free improved moving least-square Ritz (IMLS-Ritz) method to analysis the buckling behavior of functionally graded carbon nanotube (FG-CNT) reinforced composite thick skew plates on Pasternak foundations. The governing equations were derived based on the first-order shear deformation theory (FSDT). Zhang and Liew [51] studied the geometrically nonlinear large deformation analysis of FG-CNT reinforced composite skew plates rested on elastic foundations. They used the FSDT, von Karman

* Corresponding author. Department of Mechanical Engineering, Ferdowsi University of Mashhad, Mashhad 91775-1111, Iran.
E-mail address: kadkhoda@um.ac.ir (M. Kadkhodayan).

http://dx.doi.org/10.1016/j.compositesb.2017.05.070
1359-8368/

assumption and the element-free IMLS-Ritz method to derive the governing equations. Ketabdari et al. [52] used the energy and Rayleigh-Ritz methods to investigate the free vibration analysis of homogeneous and FGM skew plates rested on variable elastic foundation.

The three-dimensional thermal analysis of a FGM skew plate on elastic foundation has not been considered in the literature. Nevertheless, one of the most common applications of FGMs is in high temperatures where there is a requirement of heat and failure-resistant simultaneously. Based on the best knowledge of the authors, however, there is no work in the literature on multi-directional FGM skew plates.

New applications of FGMs in the environments that temperature varies in two or three directions (such as aerospace shuttles and craft) needs more emphasis on analyses of different structures made of multi-directional FGM such as plates [53,54].

The mechanical behaviors of structures made of multi-directional FGM under different conditions have been investigated by many researchers [55–63]. Thus, various studies were conducted on the analysis of such structures using different methods. Some researchers have used FEM for the mechanical analysis of multi directional FGM plates [53,61]. One important point in using this method is that the stress curve is not continuous over the direction which material changes. A large number of elements are also required in using this method in thermo-mechanical analysis especially in the direction which the material changes. In some studies, analytical or semi-analytical methods were used [62,63]. Several simplifying assumptions on boundary conditions, load and material distribution cause the results to be valid only under specific conditions.

The DQM is a powerful numerical method used by many researchers to analyze the different structures in the last years [64–75]. Fast convergence and accuracy of results are the most benefits of this method. On the other hand, many of papers published in the field of FG plates are based on plate theories [76] which is not very accurate for thick plates. Hence, effective numerical techniques for three dimensional analyses of FG structures can provide more accurate results as the authors [77] used the DQM to thermo-mechanical analysis of a multi-directional FGM plate based on theory of elasticity.

To the best of authors' knowledge, there is no result for the three dimensional thermo-mechanical analysis of FG skew plates on elastic foundation. Moreover, no study has been performed to analysis the multi-directional FG skew plates and there is no paper deals with dynamic response of a FG skew plate on elastic foundation.

In the current study, the three-dimensional conduction heat transfer equation is employed to estimate the temperature distribution in the skew plate. Afterwards, the temperature distribution determined in each node is used to obtain the displacement and stress distributions in the plate. Moreover, 4D DQM is used to obtain the dynamic response of FGM skew plates for the first time. The effect of different parameters on the response of skew FGM plates on elastic foundation is studied.

2. Material distributions

A skew 3D-FGM plate of length a, width b and thickness h are considered. Schematic view of the plate and the directions of η,ζ and z are illustrated in Fig. 1. If θ equals to zero, skew plate is converted to a rectangular plate. The temperature difference between the outer surfaces leads to a temperature gradient and consequently thermal stresses on plate. Young's modulus, Poisson's

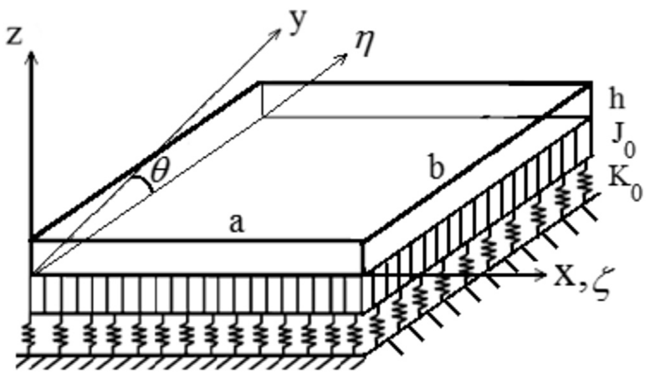

Fig. 1. 3D-FGM skew plate on elastic foundation.

ratio, density and coefficient of thermal expansion are assumed to be graded in all three spatial coordinates (η,ζ,z). The 3D-FGM skew plate is made of two constituent materials and material distribution for the plate is introduced in Eq. (1)

$$P=[P_1-P_2]V_{\eta\zeta z}+P_2 \tag{1-1}$$

$$V_{\eta\zeta z}=\left(\frac{4\eta}{a}\left(1-\frac{\eta}{a}\right)\right)^{n_\eta}\left(\frac{4\zeta}{b}\left(1-\frac{\zeta}{b}\right)\right)^{n_\zeta}\left(\frac{z}{h}\right)^{n_z} \tag{1-2}$$

where P_1 and P_2 are material parameters such as a Young's modulus and P is the property of multi-directional FGM plate. n_η, n_ζ and n_z are volume fraction exponents at η, ζ and z directions with non-negative values. By setting one, two or three volume fraction exponents equal to zero, proper equations for 2D-FGM and 1D-FGM or isotropic plate are made, respectively.

Similar to [78], all material properties are considered to be temperature-dependent excluding thermal conductivity. Considering thermal conductivities as temperature dependent parameters makes the problem nonlinear. Temperature dependencies of material parameters (e.g. Q) is considered as following [78].

$$Q(T)=Q_0\left(Q_{-1}T^{-1}+1+Q_1T+Q_2T^2+Q_3T^3\right) \tag{2}$$

$Q_i(i=-1,0,1,2,3)$ are constants and dependent on the material.

3. Governing equations

The solution process consists of two main steps, “thermal analysis” and “mechanical analysis”. The solution method is uncoupled and firstly, the steady state heat transfer analysis is performed to obtain the temperature distribution due to temperature difference between the outer surfaces of plate and then the mechanical analysis is achieved to obtain the displacements and stresses. Governing equations is derived in Cartesian coordinates (x,y,z) and then a proper variable change are used to obtain the equations for skew plate coordinates (η,ζ,z).

3.1. Thermal analysis

Three dimensional steady state heat transfer equation in absence of generation resources is as follows

$$\frac{\partial}{\partial x}\left[K_x\frac{\partial T}{\partial x}\right]+\frac{\partial}{\partial y}\left[K_y\frac{\partial T}{\partial y}\right]+\frac{\partial}{\partial z}\left[K_z\frac{\partial T}{\partial z}\right]=0 \tag{3-1}$$

in which K is the thermal conductivity. The boundary conditions are related to temperature values of outer surfaces of the plate as

$$T(x, y, 0) = T(0, y, z) = T(a, y, z) = T(x, 0, z) = T(x, b, z) = T_b \tag{3-2}$$

and

$$T(x, y, h) = 300 + (T_c - 300) \times \sin\left(\frac{\pi}{a}x\right)\sin\left(\frac{\pi}{b}y\right) \tag{3-3}$$

where T_b and T_c are constant values.

3.2. Mechanical analysis

The stress-strain relations in thermo-elastic constitutive equations can be written as follows [79].

$$\sigma_x = \frac{E}{(1+\nu)(1-2\nu)}\left[(1-\nu)\varepsilon_x + \nu(\varepsilon_y + \varepsilon_z)\right] - \frac{E}{1-2\nu}\int_{T_0}^{T} \alpha dT \tag{4-1}$$

$$\sigma_y = \frac{E}{(1+\nu)(1-2\nu)}\left[(1-\nu)\varepsilon_y + \nu(\varepsilon_x + \varepsilon_z)\right] - \frac{E}{1-2\nu}\int_{T_0}^{T} \alpha dT \tag{4-2}$$

$$\sigma_z = \frac{E}{(1+\nu)(1-2\nu)}\left[(1-\nu)\varepsilon_z + \nu(\varepsilon_x + \varepsilon_y)\right] - \frac{E}{1-2\nu}\int_{T_0}^{T} \alpha dT \tag{4-3}$$

$$\tau_{xy} = \frac{E}{(1+\nu)}\varepsilon_{xy}, \tau_{xz} = \frac{E}{(1+\nu)}\varepsilon_{xz}, \tau_{yz} = \frac{E}{(1+\nu)}\varepsilon_{yz} \tag{4-4}$$

in which T_0 is the initial temperature and T is the current temperature. The linear strain-displacement relations are defined as

$$\begin{aligned} &\varepsilon_x = \frac{\partial u}{\partial x}, \varepsilon_y = \frac{\partial v}{\partial y}, \varepsilon_z = \frac{\partial w}{\partial z} \\ &\varepsilon_{xy} = \frac{1}{2}\left(\frac{\partial u}{\partial y} + \frac{\partial v}{\partial x}\right), \varepsilon_{xz} = \frac{1}{2}\left(\frac{\partial u}{\partial z} + \frac{\partial w}{\partial x}\right), \varepsilon_{yz} = \frac{1}{2}\left(\frac{\partial v}{\partial z} + \frac{\partial w}{\partial y}\right) \end{aligned} \tag{5}$$

where u,v and w are displacement components at x, y and z directions, respectively. Equations of motion in absence of body forces are

$$\frac{\partial \sigma_x}{\partial x} + \frac{\partial \tau_{xy}}{\partial y} + \frac{\partial \tau_{xz}}{\partial z} = \rho \frac{\partial^2 u}{\partial t^2} \tag{6-1}$$

$$\frac{\partial \tau_{xy}}{\partial x} + \frac{\partial \sigma_y}{\partial y} + \frac{\partial \tau_{yz}}{\partial z} = \rho \frac{\partial^2 v}{\partial t^2} \tag{6-2}$$

$$\frac{\partial \tau_{xz}}{\partial x} + \frac{\partial \tau_{yz}}{\partial y} + \frac{\partial \sigma_z}{\partial z} = \rho \frac{\partial^2 w}{\partial t^2} \tag{6-3}$$

Combining Eq. (5) with Eq. (4) and inserting the result into Eq. (6), gives the equations of motion for three directional FGM plate in terms of displacement components as

In Eqs. (7-1) to (7-3), all properties of material (such as E and ν) in all nodes of the domain are calculated based on Eqs. (1) and (2). The boundary conditions used in this paper are defined as follows

$$\begin{aligned}
&\left(\frac{\frac{\partial E}{\partial x}(1+\nu)(1-2\nu) - E\left(\frac{\partial \nu}{\partial x}(1-2\nu) - 2\frac{\partial \nu}{\partial x}(1+\nu)\right)}{(1+\nu)^2(1-2\nu)^2}\right)\left[(1-\nu)\frac{\partial u}{\partial x} + \nu\left(\frac{\partial v}{\partial y} + \frac{\partial w}{\partial z}\right)\right] \\
&+\frac{E}{(1+\nu)(1-2\nu)}\left[-\frac{\partial \nu}{\partial x}\frac{\partial u}{\partial x} + (1-\nu)\frac{\partial^2 u}{\partial x^2} + \frac{\partial \nu}{\partial x}\left(\frac{\partial v}{\partial y} + \frac{\partial w}{\partial z}\right) + \nu\left(\frac{\partial^2 v}{\partial x \partial y} + \frac{\partial^2 w}{\partial x \partial z}\right)\right] \\
&-\frac{\frac{\partial E}{\partial x}(1-2\nu) + 2E\frac{\partial \nu}{\partial x}}{(1-2\nu)^2}\int_{T_0}^{T} \alpha dT - \frac{E}{(1-2\nu)}\frac{\partial\left(\int_{T_0}^{T} \alpha dT\right)}{\partial x} \\
&+\frac{1}{2}\frac{\frac{\partial E}{\partial y}(1+\nu) - E\frac{\partial \nu}{\partial y}}{(1+\nu)^2}\left(\frac{\partial u}{\partial y} + \frac{\partial v}{\partial x}\right) + \frac{1}{2}\frac{E}{(1+\nu)}\left(\frac{\partial^2 u}{\partial y^2} + \frac{\partial^2 v}{\partial x \partial y}\right) \\
&+\frac{1}{2}\frac{\frac{\partial E}{\partial z}(1+\nu) - E\frac{\partial \nu}{\partial z}}{(1+\nu)^2}\left(\frac{\partial w}{\partial x} + \frac{\partial u}{\partial z}\right) + \frac{1}{2}\frac{E}{(1+\nu)}\left(\frac{\partial^2 w}{\partial x \partial z} + \frac{\partial^2 u}{\partial z^2}\right) = \rho\frac{\partial^2 u}{\partial t^2}
\end{aligned} \tag{7-1}$$

$$\frac{1}{2}\frac{\frac{\partial E}{\partial x}(1+\nu)-E\frac{\partial \nu}{\partial x}}{(1+\nu)^2}\left(\frac{\partial u}{\partial y}+\frac{\partial v}{\partial x}\right)+\frac{1}{2}\frac{E}{(1+\nu)}\left(\frac{\partial^2 u}{\partial x\partial y}+\frac{\partial^2 v}{\partial x^2}\right)$$
$$+\left(\frac{\frac{\partial E}{\partial y}(1+\nu)(1-2\nu)-E\left(\frac{\partial \nu}{\partial y}(1-2\nu)-2\frac{\partial \nu}{\partial y}(1+\nu)\right)}{(1+\nu)^2(1-2\nu)^2}\right)\left[(1-\nu)\frac{\partial v}{\partial y}+\nu\left(\frac{\partial u}{\partial x}+\frac{\partial w}{\partial z}\right)\right]$$
$$+\frac{E}{(1+\nu)(1-2\nu)}\left[-\frac{\partial \nu}{\partial y}\frac{\partial v}{\partial y}+(1-\nu)\frac{\partial^2 v}{\partial y^2}+\frac{\partial \nu}{\partial y}\left(\frac{\partial u}{\partial x}+\frac{\partial w}{\partial z}\right)+\nu\left(\frac{\partial^2 u}{\partial x\partial y}+\frac{\partial^2 w}{\partial y\partial z}\right)\right] \tag{7-2}$$
$$-\frac{\frac{\partial E}{\partial y}(1-2\nu)+2E\frac{\partial \nu}{\partial y}}{(1-2\nu)^2}\int_{T_0}^{T}\alpha dT-\frac{E}{(1-2\nu)}\frac{\partial\left(\int_{T_0}^{T}\alpha dT\right)}{\partial y}$$
$$+\frac{1}{2}\frac{\frac{\partial E}{\partial z}(1+\nu)-E\frac{\partial \nu}{\partial z}}{(1+\nu)^2}\left(\frac{\partial v}{\partial z}+\frac{\partial w}{\partial y}\right)+\frac{1}{2}\frac{E}{(1+\nu)}\left(\frac{\partial^2 v}{\partial z^2}+\frac{\partial^2 w}{\partial y\partial z}\right)=\rho\frac{\partial^2 v}{\partial t^2}$$

$$\frac{1}{2}\frac{\frac{\partial E}{\partial x}(1+\nu)-E\frac{\partial \nu}{\partial x}}{(1+\nu)^2}\left(\frac{\partial u}{\partial z}+\frac{\partial w}{\partial x}\right)+\frac{1}{2}\frac{E}{(1+\nu)}\left(\frac{\partial^2 u}{\partial x\partial z}+\frac{\partial^2 w}{\partial x^2}\right)$$
$$+\frac{1}{2}\frac{\frac{\partial E}{\partial y}(1+\nu)-E\frac{\partial \nu}{\partial y}}{(1+\nu)^2}\left(\frac{\partial v}{\partial z}+\frac{\partial w}{\partial y}\right)+\frac{1}{2}\frac{E}{(1+\nu)}\left(\frac{\partial^2 v}{\partial y\partial z}+\frac{\partial^2 w}{\partial y^2}\right)$$
$$+\left(\frac{\frac{\partial E}{\partial z}(1+\nu)(1-2\nu)-E\left(\frac{\partial \nu}{\partial z}(1-2\nu)-2\frac{\partial \nu}{\partial z}(1+\nu)\right)}{(1+\nu)^2(1-2\nu)^2}\right)\left[(1-\nu)\frac{\partial w}{\partial z}+\nu\left(\frac{\partial u}{\partial x}+\frac{\partial v}{\partial y}\right)\right] \tag{7-3}$$
$$+\frac{E}{(1+\nu)(1-2\nu)}\left[-\frac{\partial \nu}{\partial z}\frac{\partial w}{\partial z}+(1-\nu)\frac{\partial^2 w}{\partial z^2}+\frac{\partial \nu}{\partial z}\left(\frac{\partial u}{\partial x}+\frac{\partial v}{\partial y}\right)+\nu\left(\frac{\partial^2 u}{\partial x\partial z}+\frac{\partial^2 v}{\partial y\partial z}\right)\right]$$
$$-\frac{\frac{\partial E}{\partial z}(1-2\nu)+2E\frac{\partial \nu}{\partial z}}{(1-2\nu)^2}\int_{T_0}^{T}\alpha dT-\frac{E}{(1-2\nu)}\frac{\partial\left(\int_{T_0}^{T}\alpha dT\right)}{\partial z}=\rho\frac{\partial^2 w}{\partial t^2}$$

$$\text{SSSS}\ \begin{cases}\zeta=0,a\rightarrow v_\eta=w=\sigma_n=0\\ \eta=0,b\rightarrow u_\zeta=w=\sigma_n=0\end{cases} \tag{8-1}$$

$$\text{CCCC}\ \begin{cases}\zeta=0,a\\ \eta=0,b\end{cases}\rightarrow u_\zeta=0,v_\eta=0,w=0 \tag{8-2}$$

$$\text{SCSC}\ \begin{cases}S:\zeta=0,a\rightarrow v_\eta=w=\sigma_n=0\\ C:\eta=0,b\rightarrow u_\zeta=v_\eta=w=0\end{cases} \tag{8-3}$$

$$\text{FCFC}\ \begin{cases}F:\zeta=0,a\rightarrow \sigma_n=\tau_{\zeta\eta}=\tau_{\zeta z}=0\\ C:\eta=0,b\rightarrow u_\zeta=v_\eta=w=0\end{cases} \tag{8-4}$$

in which σ_n is the normal stress and u_ζ and v_η are defined in appendix. 1. Boundary conditions of the top and bottom surfaces of the plate are

$$\sigma_z=q,\tau_{xz}=\tau_{yz}=0\ \text{at}\ z=h \tag{8-5}$$

$$\sigma_z=K_w w-K_{sx}\frac{\partial^2 w}{\partial x^2}-K_{sy}\frac{\partial^2 w}{\partial y^2},\tau_{xz}=\tau_{yz}=0\ \text{at}\ z=0 \tag{8-6}$$

where q is the mechanical loading and can vary through x and y directions and also $K_w=\frac{E_0K_0h^3}{a^4}, K_{sx}=\frac{\nu_0E_0J_0h^3}{a^2}, K_{sy}=\frac{\nu_0E_0J_0h^3}{b^2}$ in which $\nu_0=0.3$ and $E_0=10^9$ Pa and boundary conditions in time domain is

$$u=v=w=0\ \text{and}\ \frac{\partial u}{\partial t}=\frac{\partial v}{\partial t}=\frac{\partial w}{\partial t}=0\ \text{at t}=0 \tag{8-7}$$

For using Eqs. (7) and (8) in the skew plate the variable changes in appendix. 1 are applied.

4. Differential quadrature method (DQM)

The equations obtained in previous section are solved by a version of DQM named GDQ [11,80–82]. Relation between m^{th} time derivation of function related to x and function values in all N points of the domain is

$$\left.\frac{d^m f(x)}{dx^m}\right|_{x=x_i} = \sum_{j=1}^{N} C_{ij}^{(m)} f(x_j),\ i=1,2,\ldots,N \tag{9}$$

in which the weight coefficients for the first time and higher order derivations until N-1 are

$$C_{ij}^{(1)} = \frac{\prod_{j=1,j\neq i}^{N}(x_i-x_j)}{(x_i-x_k)\prod_{j=1,j\neq k}^{N}(x_k-x_j)},\ i,j,k=1,2,\ldots,N \tag{10-1}$$

$$C_{ii}^{(1)} = -\sum_{j=1,j\neq i}^{N} C_{ii}^{(1)},\ i=1,2,\ldots,N \tag{10-2}$$

$$C_{ij}^{(m)} = m\left[C_{ii}^{(m-1)}C_{ij}^{(1)} - \frac{C_{ij}^{(m-1)}}{x_i-x_j}\right],\quad i,\ j = 1,\ 2,\ldots,\ N \tag{10-3}$$

$$C_{ii}^{(m)} = -\sum_{j=1,j\neq i}^{N} C_{ij}^{(m)},\quad i = 1,\ 2,\ \ldots,\ N \tag{10-4}$$

where x_i (node points) is obtained from Chebyshev polynomials (l is domain length) as

$$x_i = 0.5l\left(1-\cos\left(\frac{(i-1)\times\pi}{N-1}\right)\right) \tag{11}$$

Both space and time domains are discretized based on Eq. (11). Moreover, Eq. (9) is used for all derivatives related to x, y, z and t in Eq. (7). The in-plane grid of skew plate is shown in Fig. 2.

5. Validations

To validate the results, the following comparisons with published data are performed.

5.1. Case study for mechanical analysis of a skew plate

Consider a fully clamped homogenous skew plate with the geometry and material properties as $a=0.5\text{m}, b=1\text{m}, h=0.1\text{m}, E=70\text{GPa}, \nu=0.3, \theta=30$. The plate is subjected to a uniform pressure loading $q = 20$ MPa on the top surface. Through the thickness distribution of transverse deflection are shown in Fig. 3. A good agreement between the obtained results and Ref [83] can be seen and the difference between two curves is less than 0.8%. Moreover a convergence study is shown in Table 1.

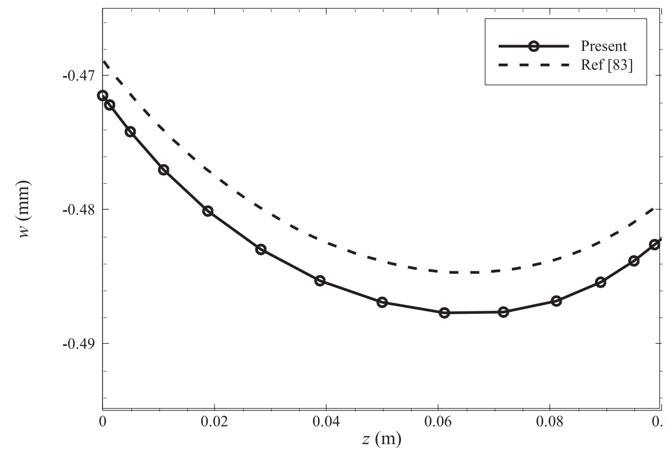

Fig. 3. Through the thickness variation of deflection of a homogenous skew plate.

5.2. Case study for thermo-mechanical analysis of a FGM rectangular plate

Consider a FGM square plate ($a = b = 10h$) with the following materials properties

$$\text{Monel}:\ K'_1 = 227.24\,GPa,\ G_1 = 65.55\,GPa,\ \alpha_1 = 15\times10^{-6}/\text{K},\ K_1 = 25\ \text{W/mK}$$

$$\text{Zirconia}:\ K'_2 = 125.83\,GPa,\ G_2 = 58.077\,GPa,\ \alpha_2 = 10\times10^{-6}/\text{K},\ K_2 = 2.09\ \text{W/mK}$$

where K', G, α and K denote bulk modulus, shear modulus, thermal expansion coefficient and thermal conductivity, respectively. The local effective material properties based on Mori-Tanaka estimates are:

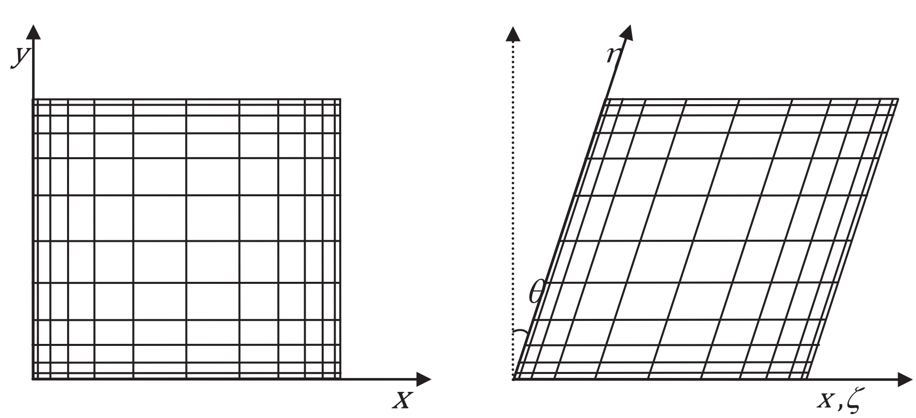

Fig. 2. A schematic in-plane grid used for skew plate.

Table 1
Convergence study of bending analysis of a skew plate.

$Nx \times Ny \times Nz$	$w(a/2, b/2, h/2)$ (mm)	$\sigma_x(a/2,b/2,0)$ (MPa)	$\tau_{xy}(a/2,b/2,0)$ (MPa)
$5 \times 5 \times 5$	−0.51324	84.83872	−25.4022
$7 \times 7 \times 7$	−0.49438	85.62554	−28.3109
$9 \times 9 \times 9$	−0.48311	80.0829	−28.497
$11 \times 11 \times 11$	−0.48797	82.49071	−28.5791
$13 \times 13 \times 13$	−0.48723	81.74038	−28.1526
$15 \times 15 \times 15$	−0.48747	82.5489	−28.4798
$17 \times 17 \times 17$	−0.48732	81.72077	−28.2284
$19 \times 19 \times 19$	−0.4874	82.51728	−28.4833

$$\frac{K'-K'_1}{K'_2-K'_1}=\frac{V_2}{1+(1-V_2)(K'_2-K')_1\Big/\left(K'_1+\frac{4}{3}G_1\right)},\quad V_2=(z/h)^{n_z}$$
$$\frac{G-G_1}{G_2-G_1}=\frac{V_2}{1+(1-V_2)(G_2-G_1)/(G_1+f_1)},\quad f_1=\frac{G_1(9K'_1+8G_1)}{6(K'_1+2G_1)}$$
$$\frac{K-K_1}{K_2-K_1}=\frac{V_2}{1+(1-V_2)(K_2-K_1)/3K_1}$$
$$\frac{\alpha-\alpha_1}{\alpha_2-\alpha_1}=\frac{\frac{1}{K'}-\frac{1}{K'_1}}{\frac{1}{K'_2}-\frac{1}{K'_1}} \tag{12}$$

Mechanical boundary conditions are SSSS with the thermal boundary conditions as:

$$\sigma_x^*=-\frac{h^2}{qa^2}\sigma_x\left(\frac{a}{2},\ \frac{b}{2},\ 0\right),\ \sigma_y^*=-\frac{h^2}{qa^2}\sigma_y\left(\frac{a}{2},\ \frac{b}{2},\ 0\right),\sigma_{xy}^*=-\frac{h^2}{qa^2}\sigma_{xy}(0,\ 0,\ 0)$$
$$w^*=\frac{100D_0}{qa^4}w\left(\frac{a}{2},\ \frac{b}{2},\ \frac{h}{2}\right),D_0=\frac{E_ch^3}{12(1-\nu^2)},\ K_0=\frac{K_wa^4}{E_0h^3},\ J_0=\frac{K_{sx}a^2\nu}{E_0h^3}=\frac{K_{sy}b^2\nu}{E_0h^3} \tag{14}$$

$$T(x,\ y,\ h)=T^+\sin\left(\frac{m_1\pi}{a}x\right)\sin\left(\frac{m_2\pi}{b}y\right)$$
$$T(x,\ y,\ 0)=T(0,\ y,\ z)=T(a,\ y,\ z)=T(x,\ 0,\ z)=T(x,\ b,\ z)=0 \tag{13}$$

Table 2 shows a comparison of non-dimensional deflection and normal stresses ($\overline{w}=\frac{w}{10^{-6}T^+a}$, $\overline{\sigma_{ij}}=\frac{\sigma_{ij}}{10^3T^+}$) with those reported in Ref. [84].

Table 2
Results for FGM square plate under thermal load ($m_1=m_2=1, a=b, a/h=10, n_x=n_y=0, n_z=2$).

	z/h	$Nx \times Ny \times Nz$				Ref. [84]
		$11 \times 11 \times 11$	$13 \times 13 \times 13$	$15 \times 15 \times 15$	$17 \times 17 \times 17$	
$\overline{w}$	1	5.4035	5.8369	5.9633	6.0016	6.021
	0.5	5.0104	5.449	5.5769	5.6156	5.635
	0	4.9039	5.3375	5.464	5.5023	5.522
$\overline{\sigma}_x$	1	−1072.3	−1025.8	−1012.2	−1008.1	−1006
	0.5	−244.5	−243.9	−243	−243	−243
	0	2.9	−52.5	−68.7	−73.6	−75.78
$\overline{\sigma}_z$	0.5	4.8555	0.8918	1.3846	1.0035	1.015

5.3. Case studies for the homogeneous and FGM rectangular plates on elastic foundation

5.3.1. Homogeneous plate

A homogeneous square thin plate ($a=b=100h$) on Winkler-Pasternak foundation is considered. The plate is subjected to a uniform load on its top surface. The obtained results for central deflection of the plate for three different boundary conditions (SSSS, SCSC and SFSF) and various foundation parameters are shown in Table 3. The non-dimensional foundation parameters k_w and k_p are defined as:

$$k_w=\frac{K_wa^4}{D},\ k_p=\frac{K_pa^2}{D}\ \text{where}\ D=Eh^3\Big/12\left(1-\nu^2\right)\ \text{and}\ K_p=K_{sx}=K_{sy}$$

Comparing these results with those reported by Huang et al. [85] and Lam et al. [86] shows a good agreement.

5.3.2. FGM plate

A simply supported FGM rectangular plate consists of aluminum and alumina is considered. The Young's modulus and Poisson's ratio of these materials are:

$$E_m=70\ \text{GPa},\ \nu_m=0.3\ \text{Aluminum}:$$

$$E_c=380\ \text{GPa},\ \nu_c=0.3\ \text{Alumina}:$$

Deflection and stress at the middle point of the plate is shown in Table 4. The parameters used here are as following with $E_0=1.0$ GPa, $\nu=0.3$:

5.4. Case study to validate the dynamic analysis

A simply supported square plate of side length $a=2$ m and thickness $h=0.01$ m made of aluminum is considered with the Young's modulus, Poisson's ratio and density of $E=70$GPa, $\nu=0.3$ and $\rho=2707\text{kg/m}^3$, respectively. A 4D DQM ($N_x \times N_y \times N_z \times N_t$) is used and Fig. 4 shows the results for the evaluation of center deflection of plate under a suddenly applied uniform load of intensity $q_0=1$MPa and its comparison with Refs. [88,89]. The non-dimensional parameters used here are:

$$w^*=70\times10^9wh\Big/\left(q_0a^2\right),\ t^*=t\sqrt{70\times10^9/(2707a^2)} \tag{15}$$

A convergence study for this problem is shown in Fig. 5.

6. Numerical results and discussions

Consider a thick FGM skew plate of side equal to $a=b=1$ m. Material distribution is according to Eq. (1) and the constituent materials are SUS304 and Si_3N_4, Table 5. The non-uniform load and temperature at the top surface of the plate are taken as

Table 3
Non-dimensional central deflection ($10^3 Dw(0.5a,\ 0.5b,\ 0.5h)/qa^4$) of a uniformly loaded homogeneous square thin plate on Winkler-Pasternak foundations ($a = b = 100h$, $\nu = 0.3$).

	k_w	k_p	$Nx \times Ny \times Nz$						
			$7 \times 7 \times 7$	$9 \times 9 \times 9$	$11 \times 11 \times 11$	$13 \times 13 \times 13$	$15 \times 15 \times 15$	Ref. [85]	Ref. [86]
SSSS	1	1	3.8492	3.8548	3.8549	3.8549	3.8549	3.8546	3.853
		3^4	0.757	0.7629	0.763	0.763	0.763	0.763	0.763
		5^4	0.1132	0.1154	0.1152	0.1153	0.1153	0.1153	0.115
SCSC	3^4	1	1.6859	1.6802	1.6961	1.6938	1.6986		1.7
		3^4	0.5697	0.5705	0.576	0.5743	0.5761		0.576
		5^4	0.1011	0.1058	0.1055	0.1052	0.1057		0.106
SFSF	5^4	1	1.6578	1.6578	1.6586	1.6589	1.6591		1.66
		3^4	0.8507	0.8533	0.853	0.8525	0.8523		0.851
		5^4	0.201	0.2032	0.2034	0.2034	0.2032		0.203

Table 4
Non-dimensional deflection and stress of uniformly loaded FGM rectangular plate with simply supported edges on elastic foundation ($b = 3a = 30h$).

n_z	K_0	J_0		w^*	σ_x^*	σ_y^*	σ_{xy}^*
0	0	0	$7 \times 7 \times 7$	1.2416	0.7052	0.231	0.267
			$9 \times 9 \times 9$	1.2554	0.7155	0.2461	0.283
			$11 \times 11 \times 11$	1.2547	−0.7155	−0.2444	0.2855
			$13 \times 13 \times 13$	1.2546	0.715	0.2443	0.286
			$15 \times 15 \times 15$	1.2545	0.7153	0.2445	0.286
			Ref. [87]	1.2583	0.716	0.2447	0.289
	100	0	$7 \times 7 \times 7$	1.2097	0.6863	0.2238	0.262
			$9 \times 9 \times 9$	1.2234	0.6965	0.2389	0.2781
			$11 \times 11 \times 11$	1.2227	0.6965	0.2372	0.2806
			$13 \times 13 \times 13$	1.2226	0.6961	0.2371	0.2811
			$15 \times 15 \times 15$	1.2226	0.6963	0.2372	0.2811
			Ref. [87]	1.226	0.6969	0.2375	0.284
	0	100	$7 \times 7 \times 7$	1.1508	0.6516	0.2107	0.2526
			$9 \times 9 \times 9$	1.1643	0.6618	0.2258	0.2687
			$11 \times 11 \times 11$	1.1637	0.6617	0.2241	0.2712
			$13 \times 13 \times 13$	1.1635	0.6613	0.224	0.2717
			$15 \times 15 \times 15$	1.1635	0.6615	0.2241	0.2717
			Ref. [87]	1.1662	0.6618	0.2245	0.2744
	100	100	$7 \times 7 \times 7$	1.1232	0.6352	0.2045	0.2483
			$9 \times 9 \times 9$	1.1366	0.6453	0.2196	0.2644
			$11 \times 11 \times 11$	1.1359	0.6453	0.2179	0.2669
			$13 \times 13 \times 13$	1.1358	0.6449	0.2178	0.2674
			$15 \times 15 \times 15$	1.1358	0.6451	0.2179	0.2674
			Ref. [87]	1.1382	0.6452	0.2183	0.27
1	0	0	$7 \times 7 \times 7$	2.494	0.3211	0.1052	0.1208
			$9 \times 9 \times 9$	2.5136	0.3247	0.1117	0.1278
			$11 \times 11 \times 11$	2.5109	0.3245	0.1109	0.1289
			$13 \times 13 \times 13$	2.5107	0.3243	0.1108	0.1291
			$15 \times 15 \times 15$	2.5106	0.3244	0.1109	0.1291
			Ref. [87]	2.5134	0.325	0.1111	0.1306
	100	0	$7 \times 7 \times 7$	2.3694	0.3042	0.0987	0.1164
			$9 \times 9 \times 9$	2.3895	0.3078	0.1052	0.1234
			$11 \times 11 \times 11$	2.3869	0.3076	0.1044	0.1245
			$13 \times 13 \times 13$	2.3866	0.3074	0.1043	0.1248
			$15 \times 15 \times 15$	2.3866	0.3075	0.1044	0.1248
			Ref. [87]	2.3875	0.308	0.1047	0.1262
	0	100	$7 \times 7 \times 7$	2.154	0.2751	0.0876	0.1085
			$9 \times 9 \times 9$	2.1749	0.2789	0.0942	0.1156
			$11 \times 11 \times 11$	2.1724	0.2787	0.0934	0.1167
			$13 \times 13 \times 13$	2.1723	0.2785	0.0933	0.117
			$15 \times 15 \times 15$	2.1722	0.2786	0.0934	0.117
			Ref. [87]	2.1703	0.2791	0.094	0.1182
	100	100	$7 \times 7 \times 7$	2.0592	0.2623	0.0827	0.1051
			$9 \times 9 \times 9$	2.0803	0.2661	0.0893	0.1122
			$11 \times 11 \times 11$	2.0779	0.2659	0.0885	0.1134
			$13 \times 13 \times 13$	2.0777	0.2657	0.0884	0.1136
			$15 \times 15 \times 15$	2.0777	0.2658	0.0885	0.1136
			Ref. [87]	2.0746	0.2663	0.0893	0.1148

$$q(\zeta,\ \eta,\ h) = -q_c \sin\left(\frac{\pi}{a}\zeta\right)\sin\left(\frac{\pi}{b}\eta\right)$$
$$T(\zeta,\ \eta,\ h) = 300 + (T_c - 300) \times \sin\left(\frac{\pi}{a}\zeta\right)\sin\left(\frac{\pi}{b}\eta\right) \tag{16}$$

and $T_0 = 300\text{K}$. The other thermal boundary conditions are

$$T(\zeta,\ \eta,\ 0) = T(0,\ \eta,\ z) = T(a,\ \eta,\ z) = T(\zeta,\ 0,\ z) = T(\zeta,\ b,\ z) = 300\text{K} \tag{17}$$

First, the influence of various power law exponents for a 3D-FGM skew plate is investigated. Through the thickness distribution of the transverse deflection and normal stress σ_x of central section of the skew plate ($\zeta = \frac{a}{2}, \eta = \frac{b}{2}$) are shown in Figs. 6–9. The boundary condition is assumed to be SSSS and $a = b = 10h$.

Variation of σ_x in the thickness direction under thermal loading for different combinations of material indices are shown in Fig. 6. The material variation over thickness direction has more effect on stress behavior compared to other two directions. The similar condition can be observed for mechanical loading, Fig. 8. On the other hand, the material variation in in-plane directions is the main factor for the variation of deflection of the plate under thermal loading. The material change in the thickness direction reduces the deflection. But, for the plate under mechanical loading, the main

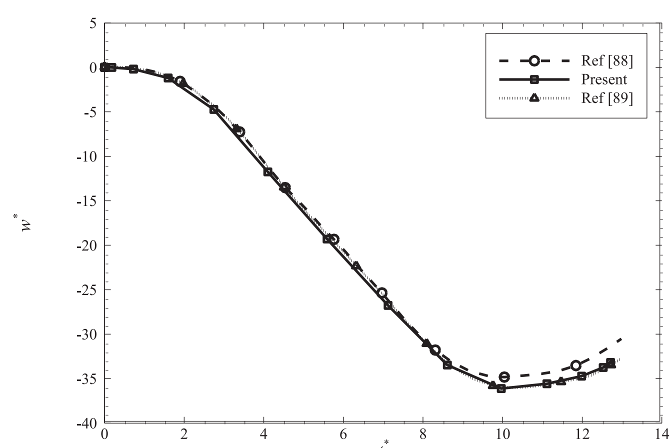

Fig. 4. Temporal evaluation of center deflection of a simply supported square plate under suddenly applied uniform loading.

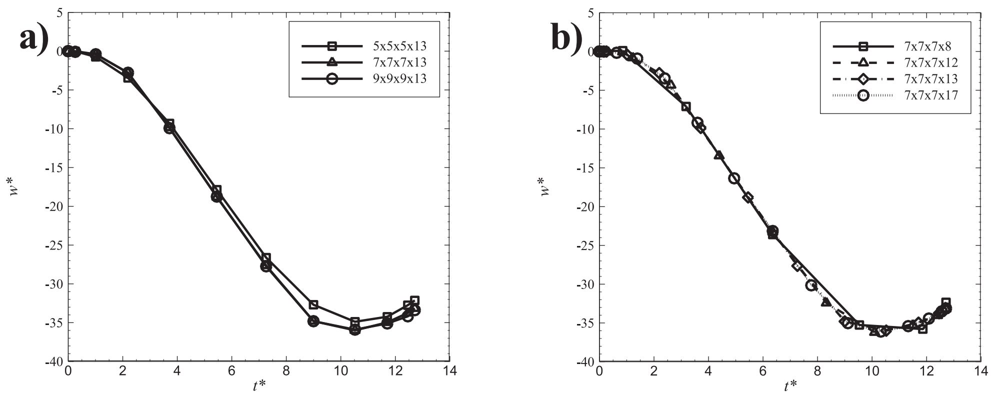

Fig. 5. Convergence study for dynamic response of the plate, (a) in space domain, (b) in time domain.

Table 5
The temperature-dependent material properties of Si_3N_4 and SUS304 [78].

Material	Property	Q_{-1}	Q_0	Q_1	Q_2	Q_3
Si_3N_4	E(Pa)	0	348.43×10^9	-3.07×10^{-4}	2.16×10^{-7}	-8.946×10^{-11}
	ν	0	0.24	0	0	0
	α(1/K)	0	5.87×10^{-6}	9.095×10^{-4}	0	0
	ρ(kg/m^3)	0	2370	0	0	0
	K(W/mK)	0	9.19	0	0	0
	c(J/kgK)	0	0.17	0	0	0
SUS304	E(Pa)	0	201.04×10^9	3.079×10^{-4}	-6.534×10^{-7}	0
	ν	0	0.3262	-2.002×10^{-4}	3.797×10^{-7}	0
	α(1/K)	0	12.33×10^{-6}	8.086×10^{-4}	0	0
	ρ(kg/m^3)	0	8166	0	0	0
	K(W/mK)	0	12.04	0	0	0
	c(J/kgK)	0	0.08	0	0	0

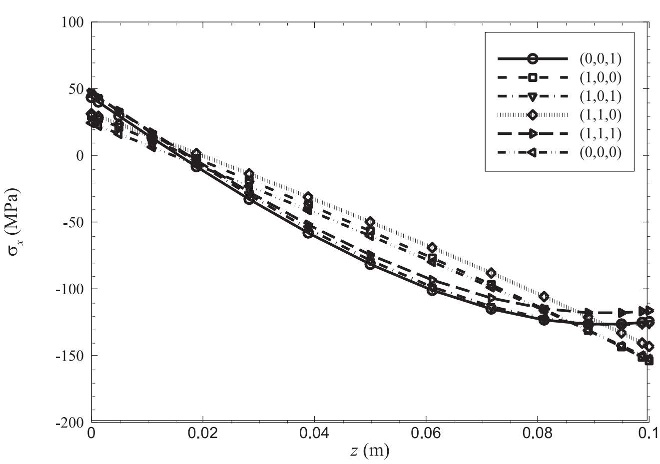

Fig. 6. Effect of power law exponents on variation of σ_x through z direction of simply supported 3D-FGM skew plate under thermal loading ($T_c = 400$ K, $q_c = 0, \theta = 30°, J_0 = K_0 = 1000$).

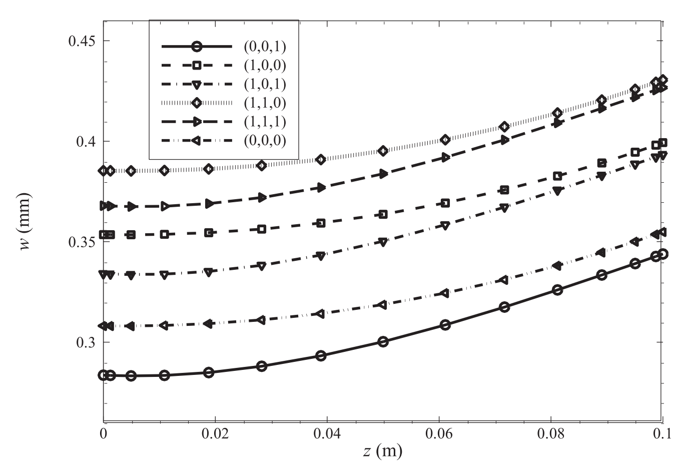

Fig. 7. Effect of power law exponents on variation of deflection through thickness of simply supported 3D-FGM skew plate under thermal loading ($T_c = 400$ K, $q_c = 0, \theta = 30°, J_0 = K_0 = 1000$).

factor of differences in deflections is the material variation through thickness direction, Fig. 9. In this case, the material variation in the in-plane directions can also increase the deflection. It is seen that the stresses and deflections of the plate strongly are affected by the directions of material variation. The obtained patterns for stresses and deflections can help designers to predict and optimize the behavior of structures.

Figs. 10–13 show the effect of boundary conditions on σ_x and the center deflection of the plate. It is observed that in both thermal and mechanical loading, the deflection decreases by increasing the constraints of the plate boundaries. As it shown in Fig. 12, the neutral plane is independent of boundary conditions of the skew plate under mechanical loading. Comparing Figs. 10 and 12, it reveals that the effect of boundary conditions on the stress is different for the plates under mechanical or thermal loading, e.g. the FCFC or SSSS cases may have higher values of stresses, see Figs. 10 and 12.

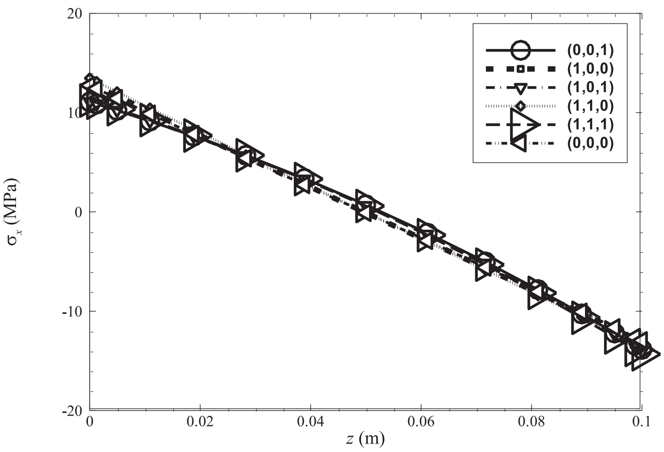

Fig. 8. Effect of power law exponents on variation of σ_x through z direction of simply supported 3D-FGM skew plate under mechanical loading ($T_c = 300$ K, $q_c = 1$MPa, $\theta = 30^\circ$, $J_0 = K_0 = 1000$).

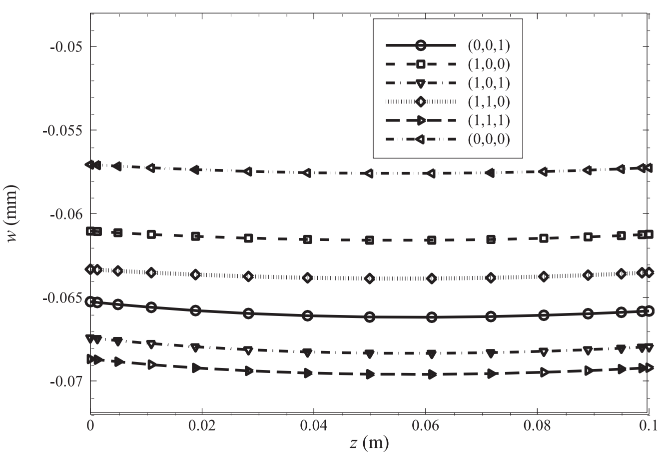

Fig. 9. Effect of power law exponents on variation of deflection through thickness of simply supported 3D-FGM skew plate under mechanical loading ($T_c = 300$ K, $q_c = 1$MPa, $\theta = 30^\circ$, $J_0 = K_0 = 1000$).

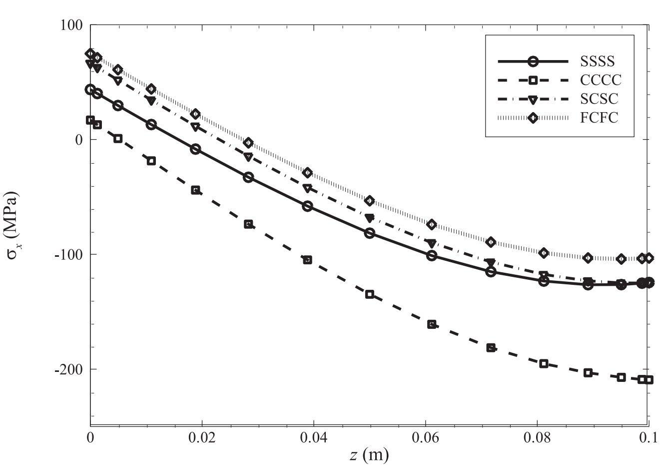

Fig. 10. Variation of σ_x through thickness of 1D-FGM plates under thermal loading for various boundary conditions ($T_c = 400$ K, $q_c = 0$, $\theta = 30^\circ$, $J_0 = K_0 = 1000$, $n_\eta = n_\zeta = 0$, $n_z = 1$).

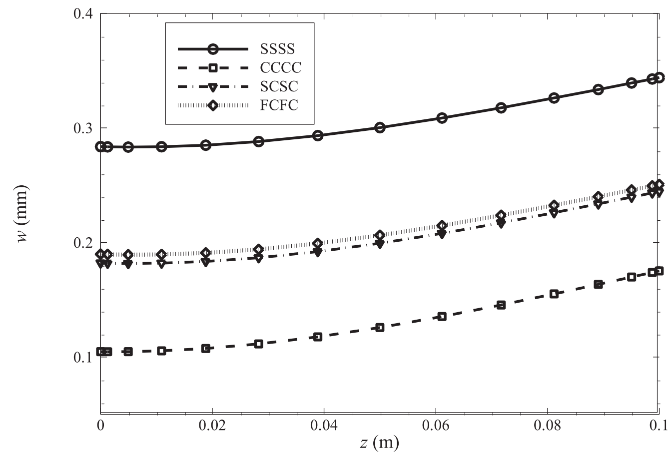

Fig. 11. Variation of deflection through thickness of 1D-FGM plates under thermal loading for various boundary conditions ($T_c = 400$ K, $q_c = 0$, $\theta = 30^\circ$, $J_0 = K_0 = 1000$, $n_\eta = n_\zeta = 0$, $n_z = 1$).

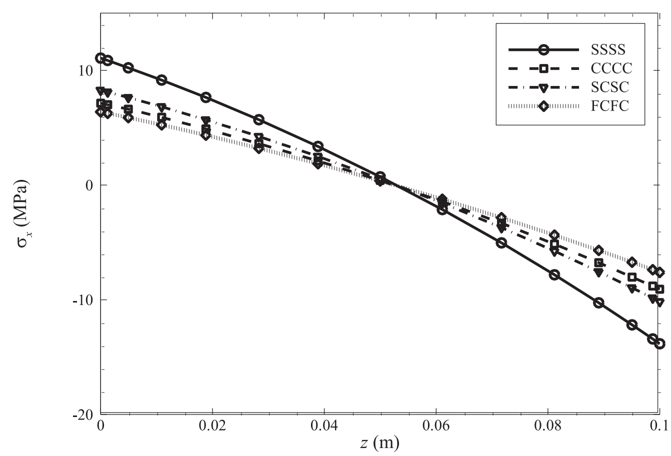

Fig. 12. Variation of σ_x through thickness of 1D-FGM plates under mechanical loading for various boundary conditions ($T_c = 300$ K, $q_c = 1$MPa, $\theta = 30^\circ$, $J_0 = K_0 = 1000$, $n_\eta = n_\zeta = 0$, $n_z = 1$).

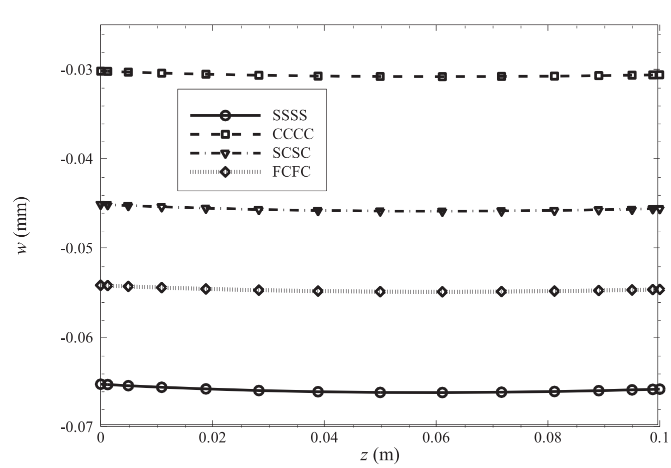

Fig. 13. Variation of deflection through thickness of 1D-FGM plates under mechanical loading for various boundary conditions ($T_c = 300$ K, $q_c = 1$MPa, $\theta = 30^\circ$, $J_0 = K_0 = 1000$, $n_\eta = n_\zeta = 0$, $n_z = 1$).

The increase of temperature at the top of the plate increases the σ_x and deflection as it was expected, Figs. 14 and 15.

In Figs. 16–19, the effects of the change of skew angle θ on stress and deflection are investigated. In the case of mechanical loading, the stress σ_x on the both top and bottom of the plate, decreases by increasing the angle, Fig. 16. Moreover, the deflection decreases by increasing the angle, Fig. 17. But the deflection curve trend of the plate under the thermal loading has a different behavior, Fig. 19.

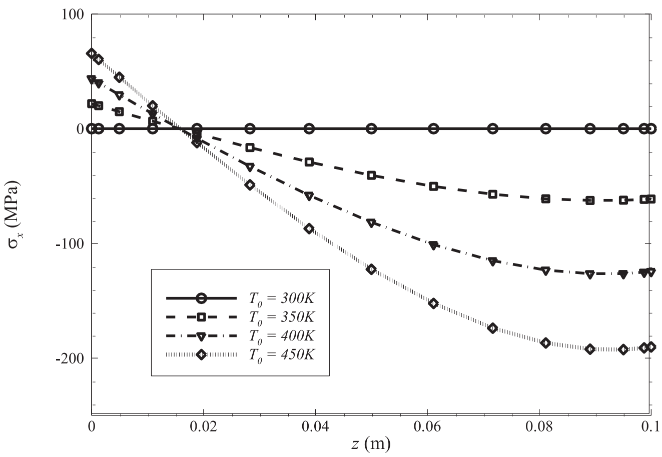

Fig. 14. Effect of thermal condition on variation of σ_x through z direction of simply supported 1D-FGM plates ($q_c = 0, \theta = 30°, J_0 = K_0 = 1000, n_\eta = n_\zeta = 0, n_z = 1$).

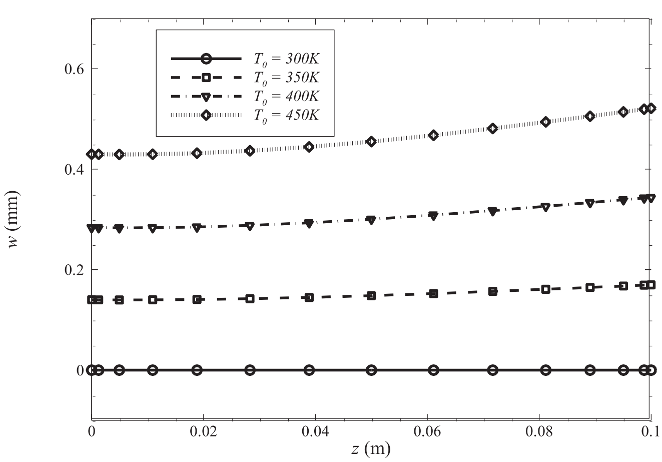

Fig. 15. Effect of thermal condition on variation of deflection through z direction of simply supported 1D-FGM plates ($q_c = 0, \theta = 30°, J_0 = K_0 = 1000, n_\eta = n_\zeta = 0, n_z = 1$).

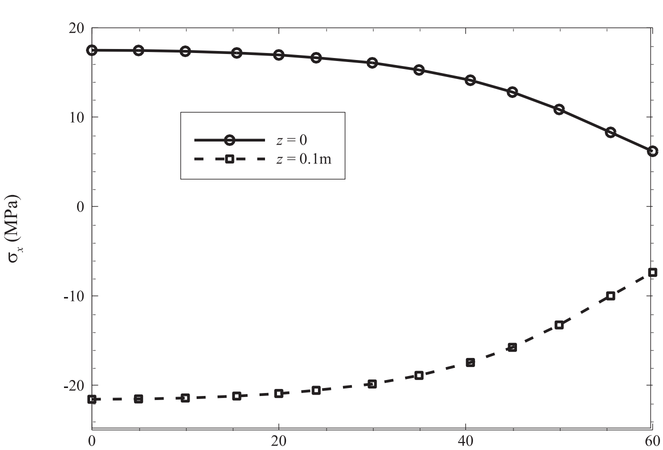

Fig. 16. Effect of skew angle on the normal stress of a 1D-FGM skew plate under mechanical loading ($T_c = 300$ K, $q_c = 1$MPa, $J_0 = K_0 = 1000, n_\eta = n_\zeta = 0, n_z = 1$).

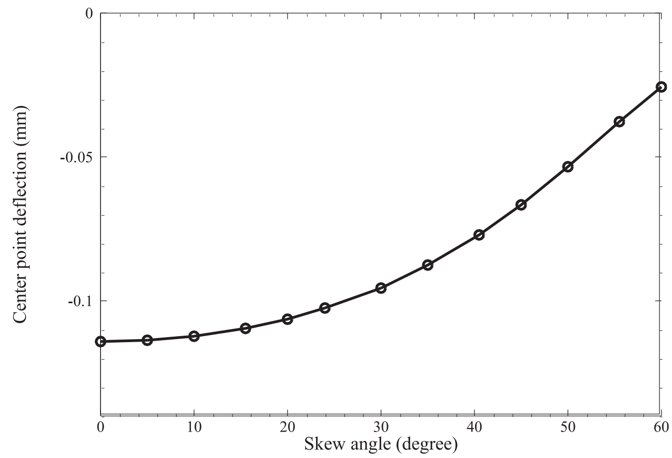

Fig. 17. Effect of skew angle on the deflection of a 1D-FGM skew plate under mechanical loading ($T_c = 300$ K, $q_c = 1$MPa, $J_0 = K_0 = 1000, n_\eta = n_\zeta = 0, n_z = 1$).

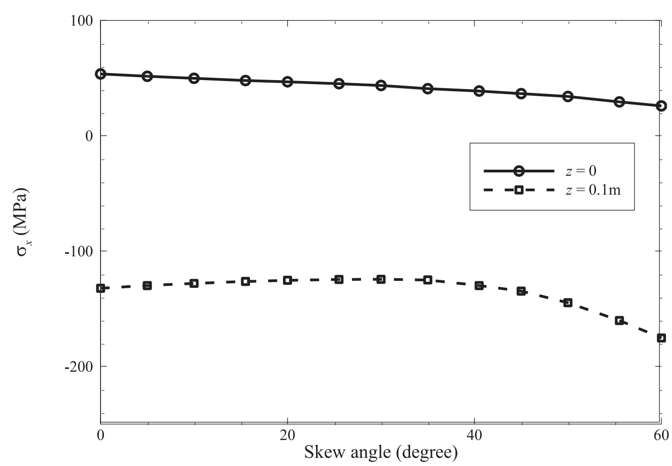

Fig. 18. Effect of skew angle on the normal stress of a 1D-FGM skew plate under thermal loading ($T_c = 400$ K, $q_c = 0, J_0 = K_0 = 1000, n_\eta = n_\zeta = 0, n_z = 1$).

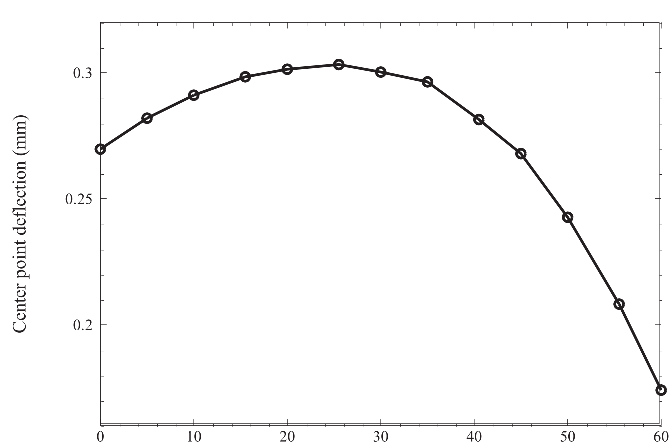

Fig. 19. Effect of skew angle on the deflection of a 1D-FGM skew plate under thermal loading ($T_c = 400$ K, $q_c = 0, J_0 = K_0 = 1000, n_\eta = n_\zeta = 0, n_z = 1$).

The stress σ_x in ($\zeta = \frac{a}{2}, \eta = \frac{b}{2}, z = 0$) decreases by increasing the angle similar to the plate under the mechanical loading although the stress in ($\zeta = \frac{a}{2}, \eta = \frac{b}{2}, z = h$) has a dissimilar behavior. Fig. 19 shows that there is an angle in which the maximum deflection of center point occurs for the simply supported skew plate on elastic foundation under thermal loading which does not happen for the case of mechanical loading, Fig. 17.

In Figs. 20–23, the effects of foundation parameters on the amount of stress and deflection are investigated. The figures indicate that in the region of analysis both σ_x and deflection are more strongly dependent upon J_0 rather than K_0 under thermal and mechanical loadings.

Figs. 24–27 show the temporal evaluation of central deflection of a multi-directional FGM skew plate under suddenly applied loading. The material variation in each direction increases the maximum deflection and its corresponding time which is due to the resulting decrease in the modulus of elasticity, Fig. 24. It is also observed that the effect of material variation in z direction on deflection history of the plate is more than that of the in-plane directions. This figure shows that one can change the transient response of a structure only with material varying in some directions and without any change in the geometry and thickness of the structure. It is an important issue especially for the aerodynamic force when the structures are designed for a special geometry and any change may cause disturbance in its performance.

It is also seen that in the region of analysis the effect of the shearing layer elastic parameter (J_0) in transient response of a FGM

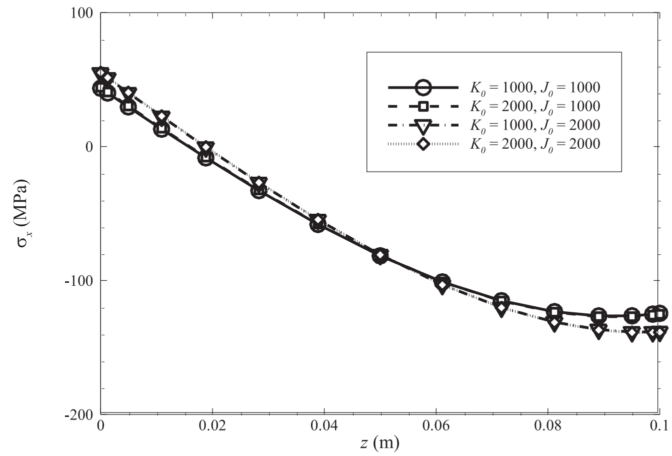

Fig. 22. Effect of foundation parameters on the normal stress of a 1D-FGM skew plate under thermal loading ($T_c = 400$ K, $\theta = 30^\circ, q_c = 0, n_\eta = n_\zeta = 0, n_z = 1$).

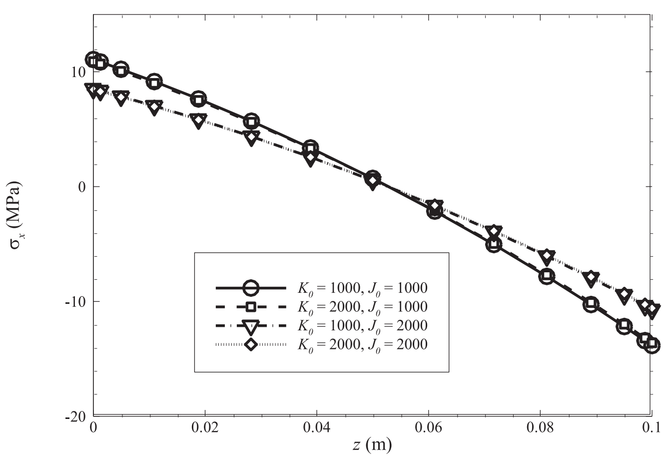

Fig. 20. Effect of foundation parameters on the normal stress of a 1D-FGM skew plate under mechanical loading ($T_c = 300$ K, $\theta = 30^\circ, q_c = 1MPa, n_\eta = n_\zeta = 0, n_z = 1$).

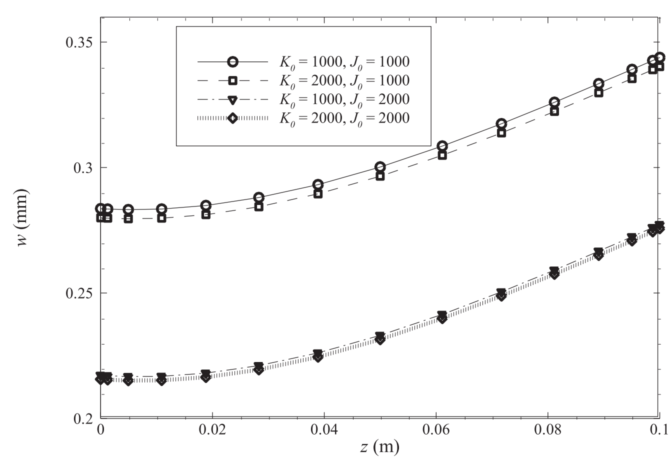

Fig. 23. Effect of foundation parameters on the deflection of a 1D-FGM skew plate under thermal loading ($T_c = 400$ K, $\theta = 30^\circ, q_c = 0, n_\eta = n_\zeta = 0, n_z = 1$).

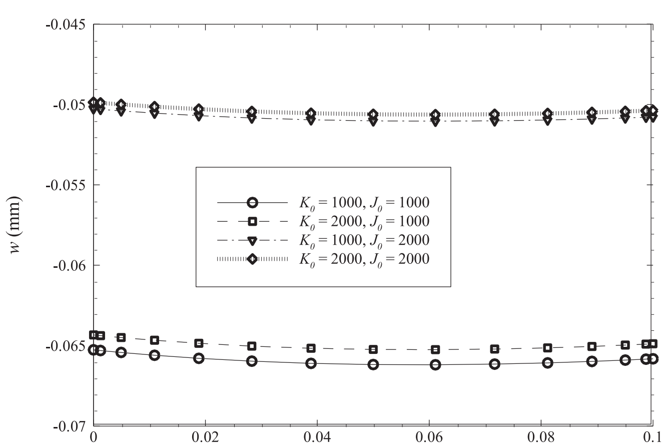

Fig. 21. Effect of foundation parameters on the deflection of a 1D-FGM skew plate under mechanical loading ($T_c = 300$ K, $\theta = 30^\circ, q_c = 1MPa, n_\eta = n_\zeta = 0, n_z = 1$).

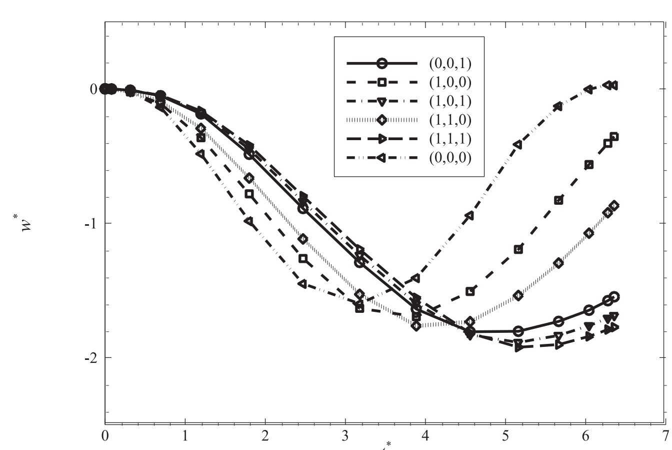

Fig. 24. Effect of grading exponents on the time history of deflection of a 1D-FGM skew plate under suddenly applied loading ($T_c = 300$ K, $\theta = 30^\circ, q_c = 1MPa, J_0 = K_0 = 1000, n_\eta = n_\zeta = 0, n_z = 1$).

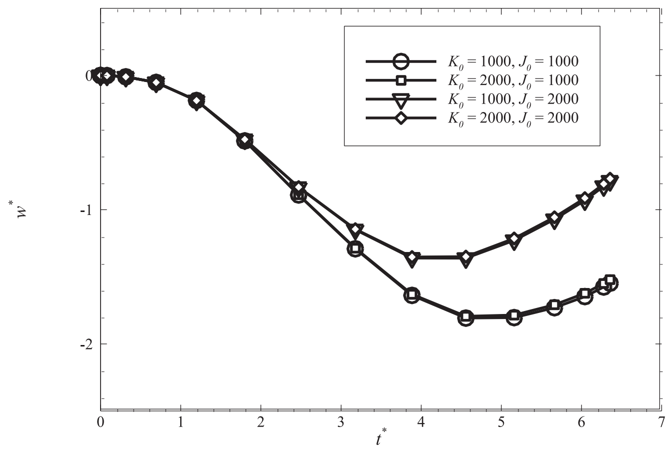

Fig. 25. Effect of foundation parameters on the time history of deflection of a 1D-FGM skew plate under suddenly applied loading ($T_c = 300$ K, $\theta = 30°$, $q_c = 1$MPa, $n_\eta = n_\zeta = 0, n_z = 1$).

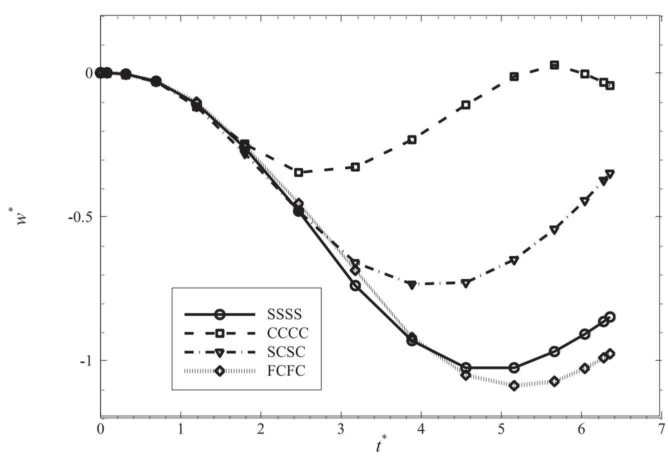

Fig. 26. Effect of boundary conditions on the time history of deflection of a 1D-FGM skew plate under suddenly applied loading ($T_c = 300$ K, $\theta = 45°$, $q_c = 1$MPa, $J_0 = K_0 = 1000, n_\eta = n_\zeta = 0, n_z = 1$).

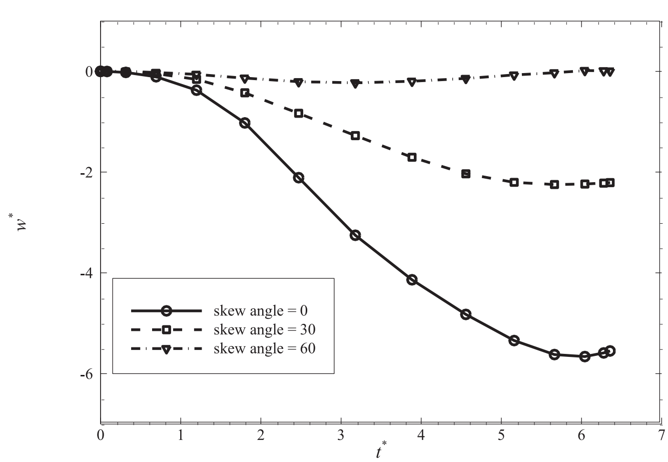

Fig. 27. Effect of skew angle on the time history of deflection of a 1D-FGM skew plate under suddenly applied loading ($T_c = 300$ K, $q_c = 1$MPa, $J_0 = K_0 = 1000, n_\eta = n_\zeta = 0, n_z = 1$).

skew plate under mechanical loading is more than that of the Winkler foundation parameter (K_0). Moreover, the increase of J_0 and K_0 reduce the maximum deflection and its corresponding time which is due to the increase of structure stiffness, Fig. 25. As expected, rising the constrains of boundaries reduces the maximum deflection and the time to reach it, Fig. 26. Moreover, it is seen that the increase of angle θ reduces the maximum deflection of transient response of FGM skew plate and its corresponding time, Fig. 27.

7. Conclusions

In this paper, three dimensional thermo-mechanical analysis of a 3D-FGM skew plate on elastic foundation was investigated for the first time. In this regard, their equations of the three dimensional theory of elasticity were derived and solved by using DQM. Additionally, 4D DQM was used to solve the equations of dynamic response of a 3D-FGM skew plate on elastic foundation. The influence of different parameters including foundation parameters, power law components and various boundary conditions on the bending behavior of FGM skew plate were presented. It is found that the direction of material gradation in a FGM skew plate has a noticeable effect on the behavior of the plate. The results also show that the power law index and the direction of material change can be used as effective parameters to design the rectangular and skew plate structures properly. It would be more important when the behavior of the structure can be enhanced with minor modification of material gradation direction without any change in the pre-design geometry of the structure obtained based on other parameters such as space limitations or aerodynamic forces. The results of the current study are determined by 3D theory of elasticity and can be employed as benchmark for other studies.

Appendix.1

Variable changes used for transforming Cartesian coordinates to skew coordinates are as follows

$$x = \zeta + \eta \sin\theta$$

$$y = \eta \cos\theta$$

$$u_\zeta = u\cos\theta - v\sin\theta$$

$$v_\eta = u\sin\theta + v\cos\theta$$

$$\frac{\partial}{\partial x} = \frac{\partial}{\partial \zeta}$$

$$\frac{\partial}{\partial y} = \frac{1}{\cos\theta}\frac{\partial}{\partial \eta} - \tan\theta\frac{\partial}{\partial \zeta}$$

$$\frac{\partial^2}{\partial x^2} = \frac{\partial^2}{\partial \zeta^2}$$

$$\frac{\partial^2}{\partial y^2} = \frac{1}{\cos^2\theta}\frac{\partial^2}{\partial \eta^2} - 2\frac{\tan\theta}{\cos\theta}\frac{\partial^2}{\partial \eta\partial \zeta} + \tan^2\theta\frac{\partial^2}{\partial \zeta^2}$$

$$\frac{\partial^2}{\partial x\partial y} = \frac{1}{\cos\theta}\frac{\partial^2}{\partial \zeta\partial \eta} - \tan\theta\frac{\partial^2}{\partial \zeta^2}$$

$$\frac{\partial^2}{\partial x\partial z} = \frac{\partial^2}{\partial \zeta\partial z}$$

$$\frac{\partial^2}{\partial y\partial z} = \frac{1}{\cos\theta}\frac{\partial^2}{\partial z\partial \eta} - \tan\theta\frac{\partial^2}{\partial z\partial \zeta}$$

References

[1] Koizumi M. FGM activities in Japan. Compos Part B 1997;28B:1–4.
[2] Jha DK, Kant T, Singh RK. A critical review of recent research on functionally graded plates. Compos Struct 2013;96:833–49.

[3] Zafarmand H, Kadkhodayan M. Three dimensional elasticity solution for static and dynamic analysis of multi-directional functionally graded thick sector plates with general boundary conditions. Compos Part B 2015;69:592–602.
[4] Malekzadeh P, Shojaee SA. Dynamic response of functionally graded plates under moving heat source. Compos Part B 2013;44:295–303.
[5] Malekzadeh P, Bahranifard F, Ziaee S. Three-dimensional free vibration analysis of functionally graded cylindrical panels with cut-out using Chebyshev–Ritz method. Compos Struct 2013;105:1–13.
[6] Zhang LW, Lei ZX, Liew KM. Free vibration analysis of FG-CNT reinforced composite straight-sided quadrilateral plates resting on elastic foundations using the IMLS-Ritz method. Epub ahead of print 2015 J Vib Control 2015. http://dx.doi.org/10.1177/1077546315587804. Published online: 6 July 2015.
[7] Farid M, Zahedinejad P, Malekzadeh P. Three-dimensional temperature dependent free vibration analysis of functionally graded material curved panels resting on two-parameter elastic foundation using a hybrid semi-analytic, differential quadrature method. Mater Des 2010;31:2–13.
[8] Malekzadeh P, Ghaedsharaf M. Three-dimensional thermoelastic analysis of finite length laminated cylindrical panels with functionally graded layers. Meccanica 2014;49:887–906.
[9] Vel SS, Batra RC. Exact solution for thermoelastic deformations of functionally graded thick rectangular plates. AIAA J 2002;40:1421–33.
[10] Vel SS, Batra RC. Three-dimensional exact solution for the vibration of functionally graded rectangular plates. J Sound Vib 2004;272:703–30.
[11] Alinaghizadeh F, Shariati M. Geometrically non-linear bending analysis of thick two-directional functionally graded annular sector and rectangular plates with variable thickness resting on non-linear elastic foundation. Compos Part B Eng 2016;86:61–83.
[12] Alinaghizadeh F, Kadkhodayan M. Large deflection analysis of moderately thick functionally graded annular sector plates fully and partially rested on two-parameter elastic foundations by GDQ method. Aerosp Sci Technol 2014;39:260–71.
[13] Alinaghizadeh F, Kadkhodayan M. Investigation of nonlinear bending analysis of moderately thick functionally graded material sector plates subjected to thermomechanical loads by the GDQ method. ASCE J Eng Mech 2014;140(5). 04014012.
[14] Fantuzzi N, Brischetto S, Tornabene F, Viola E. 2D and 3D shell models for the free vibration investigation of functionally graded cylindrical and spherical panels. Compos Struct 2016;154:573–90.
[15] Tornabene F, Brischetto S, Fantuzzi N, Bacciocchi M. Boundary conditions in 2D numerical and 3D exact models for cylindrical bending analysis of functionally graded structures. Shock Vib 2016;2016:1–17. http://dx.doi.org/10.1155/2016/2373862.
[16] Fantuzzi N, Tornabene F, Viola E. Four-parameter functionally graded cracked plates of arbitrary shape: a GDQFEM solution for free vibrations. Mech Adv Mater Struct 2015;23(1):89–107.
[17] Malekzadeh P, Monajjemzadeh SM. Dynamic response of functionally graded beams in a thermal environment under a moving load. Mech Adv Mater Struct 2015;23(3):248–58.
[18] Han SC, Park WT, Jung WY. 3D graphical dynamic responses of FGM plates on Pasternak elastic foundation based on quasi-3D shear and normal deformation theory. Compos Part B 2016;95:324–34.
[19] Liu S, Yu T, Bui TQ, Yin S, Thai DK, Tanaka S. Analysis of functionally graded plates by a simple locking-free quasi-3D hyperbolic plate isogeometric method. Compos Part B 2017;120:182–96.
[20] Yin S, Yu T, Bui TQ, Zheng X, Tanaka S. In-plane material inhomogeneity of functionally graded plates: a higher-order shear deformation plate isogeometric analysis. Compos Part B 2016;106:273–84.
[21] Farzam-Rad SA, Hassani B, Karamodin A. Isogeometric analysis of functionally graded plates using a new quasi-3D shear deformation theory based on physical neutral surface. Compos Part B 2017;108:174–89.
[22] Taczała M, Buczkowski R, Kleiber M. Nonlinear buckling and post-buckling response of stiffened FGM plates in thermal environments. Compos Part B 2017;109:238–47.
[23] Ghorbanpour Arani A, Jalaei MH. Nonlocal dynamic response of embedded single-layered graphene sheet via analytical approach. J Eng Math 2016;98(1):129–44.
[24] Asemi K, Shariyat M, Salehi M, Ashrafi H. A full compatible three-dimensional elasticity element for buckling analysis of FGM rectangular plates subjected to various combinations of biaxial normal and shear loads. Finite Elem Analysis Des 2013;74:9–21.
[25] Ansari R, Shahabodini A, Faghih Shojaei M. Nonlocal three-dimensional theory of elasticity with application to free vibration of functionally graded nanoplates on elastic foundations. Phys E Low-dimensional Syst Nanostructures 2016;76:70–81.
[26] Alibeigloo A, Pasha Zanoosi AA. Static analysis of rectangular nano-plate using three-dimensional theory of elasticity. Appl Math Model 2013;37:7016–26.
[27] Alibeigloo A, Liew KM. Thermoelastic analysis of functionally graded carbon nanotube-reinforced composite plate using theory of elasticity. Compos Struct 2013;106:873–81.
[28] Ansari R, Faghih Shojaei M, Shahabodini A, Bazdid-Vahdati M. Three-dimensional bending and vibration analysis of functionally graded nanoplates by a novel differential quadrature-based approach. Compos Struct 2015;131:753–64.
[29] Jin G, Su Z, Shi S, Ye T, Gao S. Three-dimensional exact solution for the free vibration of arbitrarily thick functionally graded rectangular plates with general boundary conditions. Compos Struct 2014;108:565–77.
[30] Vaghefi R, Baradaran GH. Koohkan, Three-dimensional static analysis of thick functionally graded plates by using meshless local Petrov–Galerkin (MLPG) method. Eng Analysis Bound Elem 2010;34:564–73.
[31] Ansari R, Ashrafi MA, Pourashraf T, Sahmani S. Vibration and buckling characteristics of functionally graded nanoplates subjected to thermal loading based on surface elasticity theory. Acta Astronaut 2015;109:42–51.
[32] Amirpour M, Das R, Flores EIS. Analytical solutions for elastic deformation of functionally graded thick plates with in-plane stiffness variation using higher order shear deformation theory. Compos Part B 2016;94:109–21.
[33] Wang YQ, Zu JW. Nonlinear dynamic thermoelastic response of rectangular FGM plates with longitudinal velocity. Compos Part B 2017;117:74–88.
[34] Nguyen TK, Nguyen VH, Chau Dinh T, Vo TP, Nguyen XH. Static and vibration analysis of isotropic and functionally graded sandwich plates using an edge-based MITC3 finite elements. Compos Part B 2016;107:162–73.
[35] Behravan Rad A, Shariyat M. A three-dimensional elasticity solution for two-directional FGM annular plates with non-uniform elastic foundations subjected to normal and shear tractions. Acta Mech Solida Sin 2013;26(6):671–90.
[36] Malekzadeh P, Safaeian Hamzehkolaei NA. 3D discrete layer-differential quadrature free vibration of multi-layered FG annular plates in thermal environment. Mech Adv Mater Struct 2013;20:316–30.
[37] Malekzadeh P, Shahpari SA, Ziaee HR. Three-dimensional free vibration of thick functionally graded annular plates in thermal environment. J Sound Vib 2010;329:425–42.
[38] Zhou D, Lo SH, Au FTK, Cheung YK, Liu WQ. 3-D vibration analysis of skew thick plates using Chebyshev–Ritz method. Int J Mech Sci 2006;48:1481–93.
[39] Zhang LW, Lei ZX, Liew KM. Buckling analysis of FG-CNT reinforced composite thick skew plates using an element-free approach. Compos Part B 2015;75:36–46.
[40] Malekzadeh P, Shojaee M. Buckling analysis of quadrilateral laminated plates with carbon nano tubes reinforced composite layers. Thin-Walled Struct 2013;71:108–18.
[41] Malekzadeh P, Setoodeh AR, Alibeygi Beni A. Small scale effect on the thermal buckling of orthotropic arbitrary straight-sided quadrilateral nanoplates embedded in an elastic medium. Compos Struct 2011;93:2083–9.
[42] Zhang LW, Lei ZX, Liew KM. Vibration characteristic of moderately thick functionally graded carbon nanotube reinforced composite skew plates. Compos Struct 2015;122:172–83.
[43] Ansari R, Shahabodini A, Faghih Shojaei M. Vibrational analysis of carbon nanotube-reinforced composite quadrilateral plates subjected to thermal environments using a weak formulation of elasticity. Compos Struct 2016;139:167–87.
[44] Vel SS, Batra RC. Exact solution for thermoelastic deformations of functionally graded thick rectangular plates. Am Inst Aeronautics Astronautics J 2002;40:1421–33.
[45] Qian LF, Batra RC. Transient thermoelastic deformations of a thick functionally graded plate. J Therm Stresses 2004;27:705–40.
[46] Vel SS, Batra RC. Three-dimensional analysis of transient thermal stresses in functionally graded plates. Int J Solids Struct 2003;40:7181–96.
[47] Bui TQ, Do TV, Ton LHT, Doan DH, Tanaka S, Pham DT, Nguyen-Van T-A, Yu T, Hirose S. On the high temperature mechanical behaviors analysis of heated functionally graded plates using FEM and a new third-order shear deformation plate theory. Compos Part B 2016;92:218–41.
[48] Li D, Deng Z, Xiao H. Thermomechanical bending analysis of functionally graded sandwich plates using four-variable refined plate theory. Compos Part B 2016;106:107–19.
[49] Joodaky A, Joodaky I, Hedayati M, Masoomi R, Borzabadi Farahani E. Deflection and stress analysis of thin FGM skew plates on Winkler foundation with various boundary conditions using extended Kantorovich method. Compos Part B 2013;51:191–6.
[50] Lei ZX, Zhang LW, Liew KM. Buckling of FG-CNT reinforced composite thick skew plates resting on Pasternak foundations based on an element-free approach. Appl Math Comput 2015;226:773–91.
[51] Zhang LW, Liew KM. Large deflection analysis of FG-CNT reinforced composite skew plates resting on Pasternak foundations using an element-free approach. Compos Struct 2015;132:974–83.
[52] Ketabdari MJ, Allahverdi A, Sayad Boreyri S, Fadavie Ardestani M. Free vibration analysis of homogeneous and FGM skew plates resting on variable Winkler-Pasternak elastic foundation. Mech Industry 2016;17. 107.
[53] Nemat-Alla M. Reduction of thermal stresses by developing two-dimensional functionally graded materials. Int J Solids Struct 2003;40:7339–56.
[54] Birman V, Chona R, Byrd LW, Haney MA. Response of spatially tailored structures to thermal loading. J Eng Math 2008;61:201–17.
[55] Qian LF, Batra RC. Design of bidirectional functionally graded plate for optimal natural frequency. J Sound Vib 2005;280:415–24.
[56] Nie GJ, Zhong Z. Dynamic analysis of multi-directional functionally graded annular plates. Appl Math Model 2010;34:608–16.
[57] Lu CF, Chen WQ, Xu RQ, Lim CW. Semi-analytical elasticity solutions for bi-directional functionally graded beams. Int J Solids Struct 2008;45:258–75.
[58] Behravan Rad A. Static analysis of two directional functionally graded circular plate under combined axisymmetric boundary conditions. Int J Eng Appl Sci 2012;4:36–48.
[59] Asgari M, Akhlaghi M, Hosseini SM. Dynamic analysis of two-dimensional functionally graded thick hollow cylinder with finite length under impact

loading. Acta Mech 2009;208:163–80.
[60] Asemi K, Salehi M, Akhlaghi M. Elastic solution of a two-dimensional functionally graded thick truncated cone with finite length under hydrostatic combined loads. Acta Mech 2011;217:119–34.
[61] Nemat-Alla M, Ahmed KIE, Hassab-Allah I. Elastic–plastic analysis of two-dimensional functionally graded materials under thermal loading. Int J Solids Struct 2009;46:2774–86.
[62] Lü CF, Lim CW, Chen WQ. Semi-analytical analysis for multi-directional functionally graded plates: 3-D elasticity solutions. Int J Numer Methods Eng 2009;79:25–44.
[63] Tahouneh V, Naei MH. A novel 2-D six-parameter power-law distribution for three-dimensional dynamic analysis of thick multi-directional functionally graded rectangular plates resting on a two-parameter elastic foundation. Meccanica 2014;49:91–109.
[64] Malekzadeh P, Golbahar Haghighi MR, Alibeygi Beni A. Buckling analysis of functionally graded arbitrary straight-sided quadrilateral plates on elastic foundations. Meccanica 2012;47:321–33.
[65] Malekzadeh P, Alibeygi Beni A. Free vibration of functionally graded arbitrary straight-sided quadrilateral plates in thermal environment. Compos Struct 2010;92:2758–67.
[66] Malekzadeh P. Three-dimensional thermal buckling analysis of functionally graded arbitrary straight-sided quadrilateral plates using differential quadrature method. Compos Struct 2011;93:1246–54.
[67] Brischetto S, Tornabene F, Fantuzzi N, Viola E. 3D exact and 2D generalized differential quadrature models for free vibration analysis of functionally graded plates and cylinders. Meccanica 2016;51:2059–98.
[68] Tornabene F, Viola E. Static analysis of functionally graded doubly-curved shells and panels of revolution. Meccanica 2013;48:901–30.
[69] Tornabene F, Fantuzzi N, Ubertini F, Viola E. Strong formulation finite element method based on differential quadrature: a survey. Appl Mech Rev 2015;67(2). http://dx.doi.org/10.1115/1.4028859. Paper No: AMR-14–1041.
[70] Ansari R, Mohammadi V, Faghih Shojaei M, Gholami R, Darabi MA. A geometrically non-linear plate model including surface stress effect for the pull-in instability analysis of rectangular nanoplates under hydrostatic and electrostatic actuations. Int J Non-Linear Mech 2014;67:16–26.
[71] Ansari R, Shahabodini A, Faghih Shojaei M, Mohammadi V, Gholami R. On the bending and buckling behaviors of Mindlin nanoplates considering surface energies. Phys E Low-dimensional Syst Nanostructures 2014;57:126–37.
[72] Ansari R, Hasrati E, Faghih Shojaei M, Gholami R, Mohammadi V, Shahabodini A. Size-dependent bending, buckling and free vibration analyses of microscale functionally graded mindlin plates based on the strain gradient elasticity theory. Lat Am J Solids Struct 2016;13(no.4).
[73] Ansari R, Gholami R, Shahabodini A. Size-dependent geometrically nonlinear forced vibration analysis of functionally graded first-order shear deformable microplates. J Mech 2016;32:539–54.
[74] Ansari R, Gholami R, Faghih Shojaei M, Mohammadi V, Darabi MA. Size-dependent nonlinear bending and postbuckling of functionally graded Mindlin rectangular microplates considering the physical neutral plane position. Compos Struct 2015;127:87–98.
[75] Ansari R, Gholami R, Faghih Shojaei M, Mohammadi V, Sahmani S. Surface stress effect on the vibrational response of circular nanoplates with various edge supports. J Appl Mech 2013;80(2):021021-1–021021–7.
[76] Swaminathan K, Naveenkumar DT, Zenkour AM, Carrera E. Stress, vibration and buckling analyses of FGM plates–A state-of-the-art review. Compos Struct 2015;120:10–31.
[77] Adineh M, Kadkhodayan M. Three-dimensional thermo-elastic analysis of multi-directional functionally graded rectangular plates on elastic foundation. Acta Mech 2017;228:881–99.
[78] Malekzadeh P, Monajjemzadeh SM. Dynamic response of functionally graded plates in thermal environment under moving load. Compos Part B 2013;45:1521–33.
[79] Advanced mechanics of materials and applied elasticity fifth ed., by Ansel Ugral and Saul Fenster.
[80] Shu C. Differential quadrature and its application in engineering. Springer; 2000.
[81] Bert CW, Malik M. Differential quadrature method in computational mechanics: a review. Appl Mech Rev 1996;49(1):1–28.
[82] Zong Z, Zhang Y. Advanced differential quadrature methods. Taylor & Francis; 2009.
[83] Asemi K, Jedari Salami S, Salehi M, Sadighi M. Dynamic and static analysis of FGM skew plates with 3D elasticity based graded finite element modeling. Lat Am J Solids Struct 2014;11:504–33.
[84] Reddy JN, Cheng ZQ. Three-dimensional thermomechanical deformations of functionally graded rectangular plates. Eur J Mech - A/Solids 2001;20:841–55.
[85] Huang ZY, Lü CF, Chen WQ. Benchmark solutions for functionally graded thick plates resting on Winkler–Pasternak elastic foundations. Compos Struct 2008;85:95–104.
[86] Lam KY, Wang CM, He XQ. Canonical exact solution for Levy plates on two parameter foundation using Green's functions. Eng Struct 2000;22:364–78.
[87] Thai HT, Choi DH. A refined plate theory for functionally graded plates resting on elastic foundation. Compos Sci Technol 2011;71:1850–8.
[88] Reddy JN. Analysis of functionally graded plates. Int J Numer Methods Eng 2000;47:663–84.
[89] Nguyen KD, Nguyen-Xuan H. An isogeometric finite element approach for three-dimensional static and dynamic analysis of functionally graded material plate structures. Compos Struct 2015;132:423–39.